Petrography-Guided Mineral Identification and Quantification - User Perspectives Based on a Multi-Laboratory Comparative Study of XRD, XRF, and FTIR

Weijun Guo[1], Shouxiang Mark Ma[2], Jennifer Kharrazi[1]

[1]Halliburton Houston Technology Center, Houston, TX, USA.
[2]Saudi Aramco, Reservoir Description Division, 31952 Dhahran, Saudi Arabia

Abstract. Mineralogy is essential for accurate reservoir characterization. The quality of laboratory testing methods - such as wavelength-dispersive X-ray fluorescence (WD-XRF), X-ray diffraction (XRD), and Fourier-transform infrared spectroscopy (FTIR) - is critical for reliable mineral quantification. This study compares results from four commercial laboratories, beginning with sample preparation and petrographic analysis, and continuing through mineralogical testing. The objective is to evaluate data quality control and provide practical guidelines from the perspective of end-users. Outcrop core samples were selected from well-characterized limestone, dolomite, sandstone, and granite formations. Each sample was first studied petrographically using scanning electron microscopy (SEM), followed by WD-XRF, XRD, and FTIR analyses by the four laboratories. Although each laboratory applied industry-standard procedures, their detailed approaches varied. Comparisons were made in three key areas: sample preparation, mineral identification, and mineral quantification. This multi-laboratory study demonstrates that petrography is essential for mineral identification, XRF delivers elemental data for XRD endpoint calibration, XRD is particularly effective for quantifying clays, quartz, and carbonates, and FTIR is best suited for rapid indicative screening. The most reliable mineralogical interpretations from integrating XRF, XRD, and FTIR data within a petrographic framework require expert collaboration for sound reservoir characterization and formation evaluation decisions.

1 Introduction

Mineralogy is a fundamental input to reservoir characterization and description, influencing decisions from well-log interpretation and geomechanical modeling to enhanced oil recovery planning. Identification and quantification of mineral assemblages - particularly clays, carbonates, and silicates - directly affect estimates of formation properties such as porosity, saturation, and permeability [1]. Four analytical methods are routinely employed by commercial rock analysis labs:

1. ***SEM-EDS*** (scanning electron microscopy with energy-dispersive X-ray spectroscopy) provides direct visual confirmation of minerals and crystal morphology, thus constrains interpretation of other indirect analytical elemental and mineralogical results.
2. ***WD-XRF*** (wavelength dispersive X-ray fluorescence) provides bulk elemental weight fractions reported as oxide percentages;
3. ***XRD*** (X-ray diffraction) identifies and quantifies crystalline mineral phases; and
4. ***FTIR*** (Fourier-transform infrared spectroscopy) detects molecular bond signatures for rapid mineral-class screening.

While each of these techniques is considered industry-standard, the specific sub-procedures adopted by individual laboratories - from sample preparation protocols and instrument calibration to software peak-fitting algorithms and mineral identification reference databases - can vary considerably [2]. This variability, largely invisible to the end-users, may introduce systematic differences in reported results that exceed the intrinsic measurement uncertainty of each method. Furthermore, the conversion of XRF elemental data to mineral weight fractions requires assumptions about mineral end-point compositions that are likewise laboratory-dependent, illustrating challenges in proper quality control of laboratory generated core data for accuracy and representativeness [3].

This study presents a multi-laboratory, multi-method comparative evaluation from the perspective of end-users who outsource mineralogical testing to commercial laboratories. Six well-characterized outcrop core samples - spanning limestone, dolomite, sandstone, and granite lithologies - were subjected to petrographic analysis using SEM-EDS, followed by WD-XRF analysis at a single reference laboratory, XRD analysis at two independent commercial laboratories, and FTIR measurements for qualitative screening (Fig. 1).

* Corresponding author: Weijun.Guo@Halliburton.com

The objectives of this study are: (a) to evaluate the reproducibility of XRD mineral quantification across different commercial providers; (b) to demonstrate the utility of cross-method elemental mass-balance validation using XRF data; and (c) to develop practical quality-control (QC) guidelines for end-users of commercial mineralogy testing services.

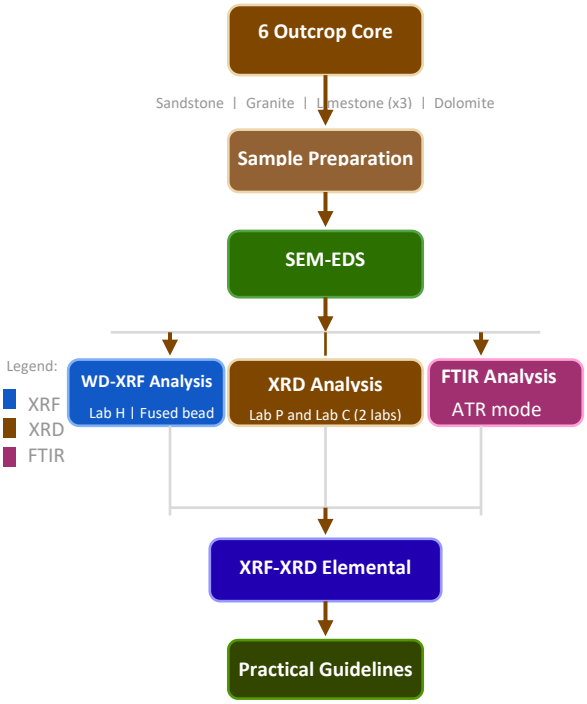

Fig. 1. Study and laboratory testing workflow.

Note that petrography by SEM-EDS serves as the interpretive ground truth throughout this study, providing direct visual confirmation of mineral species, crystal morphology, grain size, and fabric - thereby constraining interpretation of all bulk powder analytical results. The role of petrography as a guiding framework for mineral identification is a central theme, consistent with the growing recognition that optimal mineralogical characterization requires integration of multiple complementary methods, for each has its advantages and application limitations.

2 Materials and Experimental Methods

2.1 Sample Selection and Preparation

Six outcrop core samples were selected to represent contrasting mineral assemblages spanning the principal rock types in subsurface reservoir studies (Table 1):

Table 1. Sample descriptions, formation details, and analytical splits.

Sample ID	Rock Type	Formation / Lithology	Mass (g)	Analytical Splits
Massillon Sandstone	Sedimentary	Massillon Fm., Ohio | Quartz arenite	~25	XRD, WD-XRF, FTIR
Granite (8-inch core)	Igneous	Felsic plutonic | Granodiorite	~33	XRD, WD-XRF, FTIR
Vermont Marble	Metamorphic	Proctor Fm., VT | Calcite marble	~40	XRD, WD-XRF, FTIR
Kasota Dolomite	Sedimentary	Kasota Fm., MN | Dolomite-siliciclastic	~40	XRD, WD-XRF, FTIR
Cordova Cream Limestone	Sedimentary	Ordovician, TX | Near-pure calcite benchmark	~19	XRD, WD-XRF, FTIR
Indiana Limestone	Sedimentary	Salem Fm., IN | Calcite petrophysical standard	~31	XRD, WD-XRF, FTIR

This lithological diversity was intentional: contrasting mineralogy places each analytical method under different but complementary stresses, enabling method performance evaluation across the full compositional spectrum from near-monomineralic to mineralogically complex samples.

All samples were disaggregated by hand using a mortar and pestle to produce a silt-size powder passing through a 40-mesh (425-micron) sieve [2]. Upon homogenization, splits were allocated to Lab H for WD-XRF and Lab P for XRD. Because of limited sample material, splits for Lab C and FTIR testing at Lab F were obtained from a separate core piece but were homogenized to ensure analytical consistency.

2.2 SEM-EDS Petrographic Analysis

All six core samples were examined using SEM-EDS to establish petrographic ground truth prior to bulk powder analyses. Each core was cut into sections approximately 12 mm thick, placed in an aluminum dish, and dried at 105 deg C for 30 minutes to remove hygroscopic moisture. The dried sections were wrapped in conductive copper tape, sputter-coated with gold to prevent electron charging, and mounted onto the SEM stage (Fig. 2).

Fig. 2. SEM sample preparation illustration.

Image acquisition and elemental mapping by EDS characterize rock fabric, grain size and sorting, pore morphology, clay habit, and mineral associations. SEM-EDS confirmation of mineralogy provides the reference framework against which all subsequent indirect bulk analytical results were evaluated. Section 3.1 describes petrographic observations for each lithotype.

2.3 WD-XRF Elemental Analysis

WD-XRF elemental analysis was conducted at Lab H using a Bruker S8 TIGER spectrometer. With the exception of sulfur, all major and minor elements were measured using a fused-bead preparation, in which the powdered sample is mixed with a lithium tetraborate/lithium metaborate flux and melted by electric fusion. This preparation eliminates particle-size and mineralogical matrix effects. Sulfur was quantified separately by infrared combustion using a LECO instrument. Loss on ignition (LOI) was determined gravimetrically by heating to 1000 deg C.

The instrument was calibrated using a whole-rock calibration suite comprising mixed synthetic standards and certified reference materials (CRMs) with fundamental parameter optimization. Analytical accuracy was verified through replicate analyses and CRM checks; all repeat measurements showed excellent agreement with certified values. Results are reported as oxide weight percentages (wt%) plus LOI. For cross-method comparison to XRD-calculated elements, oxide concentrations were converted to elemental weight fractions using standard stoichiometric factors. Full explanation of this process can be found in the Appendix.

2.4 XRD Mineralogy Analysis

XRD analysis was performed by two laboratories:

- Lab P, using a Bruker AXS D4 diffractometer with Cu K-alpha radiation; and
- Lab C, using a Scintag Pad X or Siemens D5000 diffractometer with Cu radiation at 40 kV and 30-40 mA.

Both performed whole-rock (bulk) mineral analysis and clay-fraction mineral speciation.

Bulk sample preparation:

- Lab P employed McCrone micronizing mill grinding in ethanol, followed by spray drying into spherical aggregates loaded into stainless steel sample holders - a technique known to minimize preferred orientation and improve reproducibility.
- Lab C ground samples in isopropyl alcohol (5 min, to approximately 10 microns) and back-loaded dried powder into aluminum holders to produce random whole-rock mounts.

Clay-fraction preparation:

- Both laboratories dispersed samples in dilute sodium phosphate solution using a sonic probe, then centrifugally size-fractionated to isolate the clay-size fraction.
- Lab P collected the ≤2 micron fraction on millipore filters, glycolated at 60 deg C for a minimum of 24 hours and heat treated at 375 deg C for 1 hour to determine expandability for smectite. Oriented clay mounts were analyzed in air-dried, glycolated and heat-treated states.
- Lab C collected the ≤4 micron fraction on silver membrane filters exposed to ethylene glycol vapor for a minimum of 24 hours. Oriented clay mounts were analyzed in air-dried and glycolated states.

Measurement parameters:

- Lab P scanned 3-70 deg 2-theta at 0.02 deg step size with 1-second dwell time per step; Clay fraction scans used reduced angular ranges are 2-30 deg 2-theta. Mineral phase identification used MDI Jade 9+ software with the ICDD PDF 4+ 2024 database and Reference Intensity Ratio (RIR) peak fitting.
- Lab C scanned 2-70 deg 2-theta at 0.02 deg step at 1 deg per minute. Clay fraction scans used reduced angular ranges of 2-40 deg 2-theta. Mineral phase identification used MDI Jade 9.3 with a proprietary mixed-layer clay simulation database for determining illite/smectite expandability and ordering.

2.5 FTIR Mineralogy Analysis

FTIR was conducted at Lab F using a Bruker Alpha II spectrometer configured with a single-crystal diamond attenuated total reflectance (ATR) accessory using mid-infrared (MIR) radiation. Each measurement produced an absorbance spectrum processed using Bruker OPUS software with method-development mode to assign best-fit mineral groups.

Replicate measurements were collected for several samples to confirm reproducibility. Given the modest probing depth of ATR and sensitivity characteristics of mid-infrared methods, FTIR results are treated as qualitative to semi-quantitative indicators of mineral group presence. The method cannot reliably quantify minor phases below approximately 3-5 wt% in the presence of dominant absorbers, nor independently differentiate all polymorphs at low concentrations

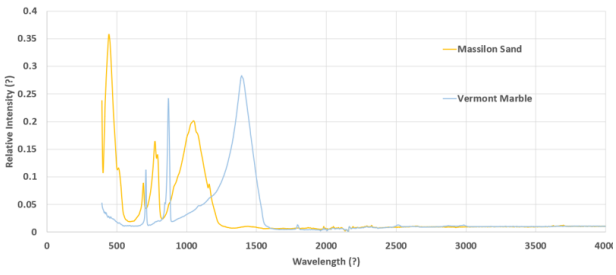

Fig. 3. Example FTIR ATR measurement spectra for sandstone and limestone.

2.6 XRF-to-XRD Elemental End-Point Framework

A mass-balance framework was established to enable cross-method validation of XRD mineral wt% against XRF elemental measurements. Stoichiometric values $C_{m,i}$, listed in Table 2 with details in the Appendix, were used to calculate the wt% of major elements from XRD.

For a sample tested, Wi is the total weight fraction of the ith element in the sample of various minerals m, the XRD-predicted elemental wt% for the ith element is:

$$W_i^{XRD} = \sum_1^{n\_m} XRD_m C_{m,i} \quad (1)$$

where XRD_m is the XRD mineral wt% normalized to 100 wt% dry weight. Refer to Appendix for details and Table 5 for example calculations of using Eq. 1

Table 2. Mineral end-point elemental compositions used for the XRF–XRD mass balance.

Mineral	Si	Al	Fe	Mg	Ca	Na	K	S
Quartz	0.467	0.000	0.000	0.000	0.000	0.000	0.000	0.000
Albite	0.321	0.103	0.000	0.000	0.000	0.088	0.000	0.000
K-feldspar	0.303	0.097	0.000	0.000	0.000	0.000	0.140	0.000
Calcite	0.000	0.000	0.000	0.000	0.400	0.000	0.000	0.000
Dolomite	0.000	0.000	0.000	0.132	0.217	0.000	0.000	0.000
Siderite	0.000	0.000	0.482	0.000	0.000	0.000	0.000	0.000
Pyrite	0.000	0.000	0.465	0.000	0.000	0.000	0.000	0.535
Chlorite	0.135	0.087	0.196	0.110	0.000	0.000	0.000	0.000
Kaolinite	0.218	0.209	0.000	0.000	0.000	0.000	0.000	0.000
Smectite (Mont.)	0.306	0.123	0.000	0.022	0.000	0.021	0.000	0.000
Illite	0.241	0.150	0.028	0.012	0.000	0.000	0.079	0.000
Hornblende	0.245	0.090	0.048	0.058	0.025	0.012	0.010	0.000

Values in g element per g mineral (from stoichiometry and literature); these end-points convert XRD mineral wt% to predicted elemental wt% for cross-validation against WD-XRF.

Color key: Blue = silicate framework minerals | Yellow-orange = carbonate minerals | Green = clay minerals

3 Experimental Results

3.1 Petrographic Observations

SEM-EDS petrography directly confirmed the compositional character of each sample and provided the reference framework against which all other indirect bulk analytical results were evaluated (Fig. 4).

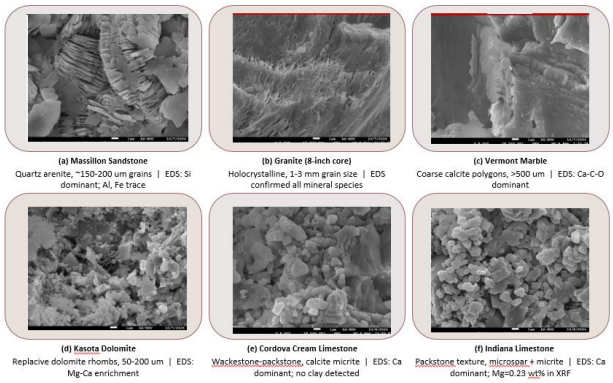

Fig. 4. SEM-EDS petrographic observations – all six lithotypes. SEM images acquired on gold-coated sections. EDS elemental mapping confirmed mineralogy.

Massillon Sandstone: A fine-to-medium-grained quartz arenite with angular to sub-rounded monocrystalline quartz grains (D50 approximately 150-200 microns) and moderate sorting (Fig. 4a). Intergranular cement is predominantly silica overgrowths, with trace kaolinite in booklet and vermicular habits indicating diagenetic precipitation. EDS mapping confirms a Si-dominated composition with subordinate Al (feldspar and clay) and trace Fe (iron oxide coatings). Mineralogy: quartz approximately 96 wt%, feldspar about 2 wt%, clay around 2 wt%.

Granite: A typical granitic holocrystalline texture with interlocking plutonic minerals averaging 1-3 mm in grain size (Fig. 4b). Quartz as anhedral strained grains (approximately 37 wt%); K-feldspar as perthitic orthoclase or microcline (about 28 wt%); plagioclase as tabular grains with polysynthetic twinning (~20 wt%); biotite/mica partially chloritized (~9 wt%); hornblende amphibole (~5 wt%); minor pyroxene (~2 wt%). The coarse-grained, heterogeneous nature of this sample has implications for representative subsampling for XRD analysis, to be discussed in Section 4.3.

Vermont Marble: Coarse-grained monomineralic calcite marble with interlocking calcite polygons (average grain size greater than 500 microns) and negligible visible porosity (Fig. 4c). SEM-EDS confirms Ca-C-O dominance, consistent with greater than 96 wt% calcite. Trace Si and K signals at grain boundaries reflect minor quartz or mica at sub-percent levels - consistent with XRF SiO2 = 0.49 wt%.

Kasota Dolomite: Replacive dolomite rhombs (50-200 microns) are the dominant phase (approximately 83 wt%), interspersed with corroded quartz grains and minor K-feldspar, plagioclase, and mixed-layer illite/smectite clay (Fig. 4d). EDS mapping shows Mg-Ca enrichment with locally variable Mg/Ca ratios at grain margins suggesting incipient ankeritic substitution.

Cordova Cream and Indiana Limestone: Wackestone to packstone textures composed predominantly of interlocking calcite micrite and minor microspar (Figs. 4e-f). Rare detrital quartz silt grains constitute less than 1 wt% of each sample. No clay minerals were detected by EDS mapping for either sample.

3.2 WD-XRF Results

Measured oxides from WD-XRF analysis are reported in Table 3 and summarized below by lithotype. All numbers are dry weight percentages. Oxides have been converted to elemental percentages by the process described in the Appendix and are reported in Table 3.

Massillon Sandstone: SiO2 = 97.83% which confirms the near-orthoquartzite description. Other minor components are Al2O3 = 1.18% from feldspars and clays and Fe2O3 = 0.23% from clay and pyrite.

Granite: SiO2 = 69.55%, Al2O3 = 14.53%, K20 = 6.98%, Na2O = 3.12% and Fe2O3 = 3.22%. There are minor amounts of other oxides.

Vermont Marble: CaO = 55.65% and LOI = 43.03% (CO2 from calcite decomposition at 1000 deg C). There are minor amounts of SiO2 and MgO.

Kasota Dolomite: CaO = 25.13%, MgO = 17.13%, and LOI = 39.44 %, all from dolomite. SiO2 = 13.72%, Al2O3 = 2.26% and K2O = 1.84% from siliciclastics.

Cordova Cream Limestone: CaO = 55.57% and LOI = 43.58%. There are minor amounts of SiO2 and MgO.

Indiana Limestone: CaO = 55.13% and LOI = 43.63%, with minor amounts of SiO2 and MgO.

Note that CRM verification confirmed all XRF repeat analyses within ±0.1wt% of certified values for major elements.

Table 3. WD-XRF analysis results – all six samples. All values in wt%. LOI = loss on ignition at 1000 °C. Oxides reported from fused-bead WD-XRF; S by LECO IR combustion. Elemental values converted from oxides.

Part A - Oxide wt%

Sample	SiO2	Al2O3	Fe2O3	MgO	CaO	K2O	Na2O	TiO2	SO3	LOI
Massillon Sand	97.83	1.18	0.23	0.01	0.02	0.27	<0.01	0.09	0.02	0.59
Granite	69.55	14.53	3.22	0.36	1.11	6.98	3.12	0.37	0.04	0.45
Vermont Marble	0.49	0.14	0.04	0.32	55.65	0.06	<0.01	0.01	0.01	43.03
Kasota Dolomite	13.72	2.26	0.43	17.13	25.13	1.84	0.04	0.08	0.06	39.44
Cordova Cream	0.25	0.07	0.13	0.36	55.57	0.02	0.01	<0.01	0.06	43.58
Indiana Lime	0.67	0.08	0.14	0.38	55.13	0.02	0.01	<0.01	0.07	43.63

Part B - Elemental wt% (converted from oxides for XRF-XRD comparison)

Sample	Si	Ti	Al	Fe	Mg	Ca	Na	K	S	Sum
Massillon Sand	45.74	0.05	0.62	0.16	0.01	0.01	--	0.22	0.01	46.82
Granite	32.52	0.22	7.69	2.25	0.22	0.79	2.31	5.79	0.02	51.81
Vermont Marble	0.23	0.01	0.07	0.03	0.19	39.78	--	0.05	0.00	40.36
Kasota Dolomite	6.41	0.05	1.20	0.30	10.33	17.96	0.03	1.53	0.02	37.83
Cordova Cream	0.12	--	0.04	0.09	0.22	39.72	0.01	0.02	0.02	40.24
Indiana Lime	0.31	--	0.04	0.10	0.23	39.41	0.01	0.02	0.03	40.15

Note: CRM verification confirmed all major elements within +/-0.1 wt% of certified values. BaO=0.12 in granite; other minor oxides omitted for brevity.

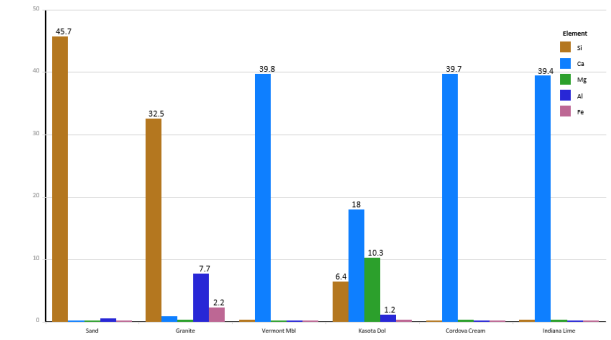

Fig. 5. WD-XRF major element comparison – selected elements by sample. Grouped bars show Si, Ca, Mg, Al and Fe elemental wt% measured by WD-XRF for each lithotype. Note the different dominant element per lithotype.

3.3 XRD Results

XRD results from Lab P and Lab C are compared by lithotype in Tables 4a and 4b and summarized below. All percentages are dry weights.

Massillon Sandstone (Lab P only): Composed predominately of Quartz with 96.0%. Minor amounts of feldspars and clays, and no carbonates.

There is excellent agreement between XRD and XRF, with Si calculated from XRD at 45.99% and measured Si from XRF at 45.74% (0.25% difference).

Granite (Lab P): Quartz 36.8%, K-feldspar 27.6%, plagioclase 20.3%, illite/mica 9.1%, amphibole 4.6%, pyroxene 1.6%. (Lab C results showed significantly different mineral distribution - attributed to sample heterogeneity, Section 3.5). Calculating elements from XRD for this lithotype is challenging because of variations in amphibole and pyroxene end-point compositions.

Vermont Marble: Lab P - calcite 96.8%, quartz 3.2%, and trace feldspars and illite/mica. Lab C - calcite 98.2%, quartz 0.8%, illite 1.1%. Calcite inter-laboratory difference: 1.4%; quartz difference: 2.4% (largest among limestone samples). Grain density: Lab P = 2.716 g/cm3; Lab C = 2.713 g/cm3 (difference 0.003 g/cm3).

Kasota Dolomite (Lab P): Dolomite 82.6%, quartz 7.5%, K-feldspar 4.1%, plagioclase 3.7%, illite/mica 1.3%, mixed illite/smectite 0.8%. (Lab C showed lower siliciclastic and slightly higher dolomite, detailed cross-comparison in Section 3.5).

Cordova Cream Limestone: Lab P - calcite 97.8%, quartz 2.2%. Lab C - calcite 99.5%, quartz 0.4%, trace illite, pyrite 0.1%. Calcite difference: 1.7% (largest of all three limestone comparisons). Grain density: Lab P = 2.709 g/cm3; Lab C = 2.712 g/cm3.

Indiana Limestone: Lab P - calcite 97.4%, quartz 2.6%. Lab C - calcite 98.8%, quartz 1.0%, illite 0.2%. Calcite difference: 1.4%; quartz difference: 1.6%. Grain density: Lab P = 2.708 g/cm3; Lab C = 2.710 g/cm3.

Across all three limestone samples, Lab P consistently reports 1.4-2.4% more quartz than Lab C. The significance of this pattern is evaluated through elemental mass-balance in Section 3.5.

Table 4a. XRD mineral quantification – Lab P (all six samples).

Bruker AXS D4, Cu K-alpha; spray-dried bulk; <2 micron clay fraction; MDI Jade 9+ / ICDD PDF4+ 2024. Values in dry mineral wt%. Tr = trace (<0.5 wt%).

Sample	Quartz	K-spar	Plag.	Calcite	Dolomite	Chlorite	Kaolinite	Illite/ Mica	Mx I/S	Amphibole	Pyroxene	GrDen (g/cc)
Massillon Sand	96.0	1.2	0.7	0.0	0.0	Tr	0.9	1.2	Tr	0.0	0.0	2.656
Granite	36.8	27.6	20.3	0.0	0.0	0.0	0.0	9.1	0.0	4.6	1.6	2.644
Vermont Marble	3.2	Tr	Tr	96.8	0.0	0.0	0.0	Tr	0.0	0.0	0.0	2.716
Kasota Dolomite	7.5	4.1	3.7	0.0	82.6	0.0	0.0	1.3	0.8	0.0	0.0	2.850
Cordova Cream	2.2	0.0	0.0	97.8	0.0	--	--	--	--	0.0	0.0	2.709
Indiana Lime	2.6	0.0	0.0	97.4	0.0	--	--	--	--	0.0	0.0	2.708

Table 4b. XRD inter-laboratory comparison – limestone and dolomite.

Sample / Lab	Quartz	K-spar	Plag	Calcite	Dolomite	Total Clay	Pyrite	GrDen (g/cc)
Vermont Marble	3.2 ***	Tr	Tr	96.8	0.0	Tr	0.0	2.716
Vermont Marble	0.8	0.0	0.0	98.2	0.0	1.1	0.0	2.713
Kasota Dolomite	7.5	4.1	3.7	0.0	82.6	2.1	0.0	2.850
Kasota Dolomite	2.2 ***	0.0	0.0	0.0	86.4	0.6	0.1	2.855
Cordova Cream	2.2	0.0	0.0	97.8	0.0	0.0	0.0	2.709
Cordova Cream	2.6 ***	0.0	0.0	99.5	0.0	0.0	0.1	2.712
Indiana Lime	2.6	0.0	0.0	97.4	0.0	0.0	0.0	2.708
Indiana Lime	1.0	0.0	0.0	98.8	0.0	0.2	0.0	2.710

Orange rows = Lab P | Green rows = Lab C | *** = exceeds XRF Si constraint

Grain density calculated from mineral assemblage using published mineral densities (quartz 2.65, calcite 2.71, dolomite 2.87 g/cc)

Key finding: Lab P quartz values in near-pure calcite samples are 1.4 to 2.4 wt% higher than Lab C; XRF Si data confirm Lab C values are likely more accurate.

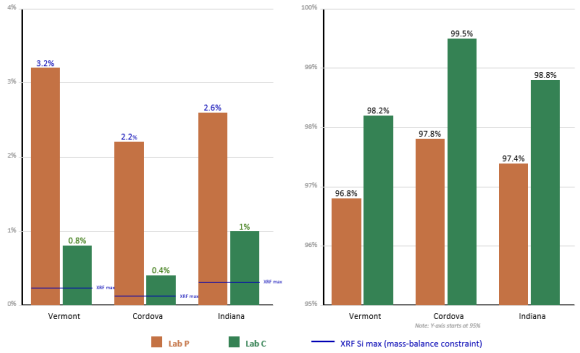

Fig. 7. XRD mineral quantification, Lab P vs. Lab C – limestone samples. Side-by-side comparison of quartz and calcite wt% for three near-pure calcite samples. Lab P systematically overestimates quartz; normalization causes a matching calcite underestimate.

3.4 FTIR Results

FTIR ATR spectra were collected and compared qualitatively against XRD mineral identifications (Figs. 3, 6).

Calcite-Dominated Samples (Vermont Marble, Cordova Cream, Indiana Limestone): All exhibit dominant absorption bands at 1400-1490 cm-1 (asymmetric nu3 CO3 stretch), 875 cm-1 (out-of-plane nu2 bending), and 712 cm-1 (in-plane nu4 bending) - characteristic of calcite. The characteristic double band at approximately 875/712 cm-1 is clearly resolved in all three spectra. No dolomite-specific band shift was detected, confirming the low Mg content.

Kasota Dolomite: Shifted carbonate band positions relative to pure calcite, with the nu3 band near 1440 cm-1 and the nu2 band displaced to approximately 879 cm-1 - consistent with Mg-Ca carbonate (dolomite). Weak silicate features near 1080 cm-1 reflect quartz and feldspar content identified by XRD.

Massillon Sandstone: Dominant Si-O stretching at approximately 1080 cm-1 and 796 cm-1, plus Si-O bending at 455 cm-1 - characteristic of quartz. Minor shoulders near 3620 cm-1 and approximately 1005 cm-1 are attributable to Al-OH kaolinite absorptions, consistent with the 0.9% kaolinite reported by XRD.

Granite: Complex multi-silicate spectrum with overlapping quartz, feldspar, and mica absorptions. Individual phase quantification is not possible by FTIR for this sample.

Notes: Replicate FTIR spectra (Fig. 6) demonstrated excellent measurement reproducibility: repeat analyses showed peak position agreement within ±2 cm-1 and absorbance intensity agreement within ±3%. However, the method cannot detect minor phases below approximately 3-5% in the presence of dominant absorbers.

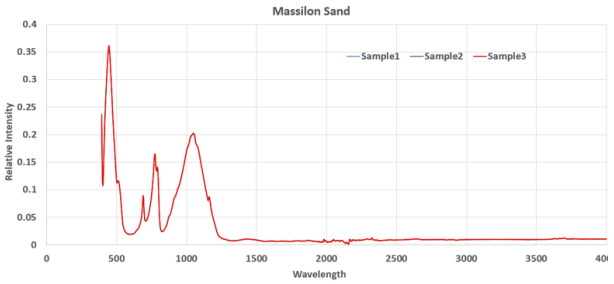

Fig. 6. Replicate FTIR spectra demonstrating measurement reproducibility.

3.5 Cross comparison and mass balance analysis

XRF and XRD are two independent measurements that can be related using known elemental compositions of minerals, thus they can be used to cross validate each other. This is done by calculating the elemental contributions of each mineral from XRD based on endpoint compositions (Section 2.6) and summing them to compare to measured XRF elemental fractions. Results are summarized below and shown in Table 5. Detailed examples of calculations are provided in the Appendix.

Massillon Sandstone: XRF Si = 45.74%; Lab P XRD-calc-Si = 45.99%; Lab C XRD-calc-Si = 45.87%. Both XRD labs overestimate Si by 0.1-0.3%, within combined uncertainty. Al, Fe, and K show good cross-method agreement. Best overall cross-method agreement of all six samples.

Granite: XRF Si = 32.52%; Lab P XRD-calc-Si = 30.02% (2.5% low); Lab C XRD-calc-Si = 25.16% (7.4% difference). Al: XRF = 7.69% vs. Lab P 5.92% and Lab C 7.07%. Larger inter-laboratory discrepancy (more than 10% total elemental mismatch) is attributed to physical sampling heterogeneity in this phaneritic rock, where different split portions were allocated to each laboratory.

Vermont Marble: XRF Si = 0.23%, implying maximum possible quartz of 0.23 / 0.467 = 0.49% (all Si in quartz). Lab P XRD reports 3.2% quartz, giving predicted Si = 1.67% - more than seven times the XRF maximum. This is physically inconsistent and confirms Lab P significantly overestimates quartz in this sample. Lab C reports 0.8% quartz (predicted Si = 0.39%) - close to but slightly above the XRF constraint, within uncertainty from minor illite (1.1%) contributing Si.

Kasota Dolomite: XRF Si = 6.41%; Lab P XRD-calc- Si = 6.44% - excellent agreement (0.03% difference). Lab C XRD-calc- Si = 4.58% - approximately 1.8% below XRF, suggesting Lab C underestimates siliciclastic minerals. Mg cross-check: XRF Mg = 10.33%; Lab P XRD Mg = 10.93%; Lab C XRD Mg = 11.61%. Both laboratories overestimate Mg, suggesting the ideal dolomite end-point overestimates Mg content (possibly reflecting partial ankeritic substitution).

Cordova Cream Limestone: XRF Si = 0.12%, maximum quartz = 0.25%. Lab P reports 2.2% quartz (predicted Si = 1.03%, more than eight times XRF). Lab C reports 0.4% quartz (predicted Si = 0.19%) - consistent with XRF. Ca:

XRF = 39.72%; Lab P = 39.12%; Lab C = 39.80%. Lab C agrees closely with XRF on both Si (quartz) and Ca (calcite).

Indiana Limestone: XRF Si = 0.31%, maximum quartz = 0.67%. Lab P reports 2.6% quartz (predicted Si = 1.21%, approximately four times XRF). Lab C reports 1.0% quartz (predicted Si = 0.52%) - slightly above XRF constraint but within compound uncertainty from multiple minor silicate phases. Ca: XRF = 39.41%; Lab P = 38.96%; Lab C = 39.52%. Lab C shows better Ca agreement.

Table 5. XRF–XRD elemental mass-balance cross-validation (key elements).

XRF = measured elemental wt%; XRD:P = Lab P calculated; XRD:CL = Lab C calculated. Red = XRD exceeds XRF by >0.3 wt% (mass-balance violation). Green = good agreement.

	Sample / Source	Si (wt%)	Al (wt%)	Fe (wt%)	Mg (wt%)	Ca (wt%)	K (wt%)	S (wt%)
Mass. Sand	XRF	45.74	0.62	0.16	0.01	0.01	0.22	0.01
	Lab P Calc.	45.99	0.61	0.17	0.04	0.00	0.28	0.11
	Lab C Calc.	45.87	0.57	0.04	0.02	0.00	0.20	0.00
Granite	XRF	32.52	7.69	2.25	0.22	0.79	5.79	0.02
	Lab P Calc.	30.02	5.92	2.69	1.16	1.00	4.64	0.00
	Lab C Calc.	25.16	7.07	3.55	1.63	0.93	5.25	0.00
Vermont Marble	XRF	0.23	0.07	0.03	0.19	39.78	0.05	0.00
	Lab P Calc.	1.67	0.07	0.01	0.00	38.72	0.04	0.00
	Lab C Calc.	0.64	0.17	0.03	0.01	39.28	0.09	0.00
Kasota Dol.	XRF	6.41	1.20	0.30	10.33	17.96	1.53	0.02
	Lab P Calc.	6.44	1.09	0.06	10.93	17.92	0.74	0.00
	Lab C Calc.	4.58	0.56	0.07	11.61	19.15	0.71	0.05
Cordova Cream	XRF	0.12	0.04	0.09	0.22	39.72	0.02	0.02
	Lab P Calc.	1.03	0.00	0.00	0.00	39.12	0.00	0.00
	Lab C Calc.	0.19	0.00	0.05	0.00	39.80	0.00	0.05
Indiana Lime	XRF	0.31	0.04	0.10	0.23	39.41	0.02	0.03
	Lab P Calc.	1.21	0.00	0.00	0.00	38.96	0.00	0.00
	Lab C Calc.	0.52	0.03	0.01	0.00	39.52	0.02	0.00

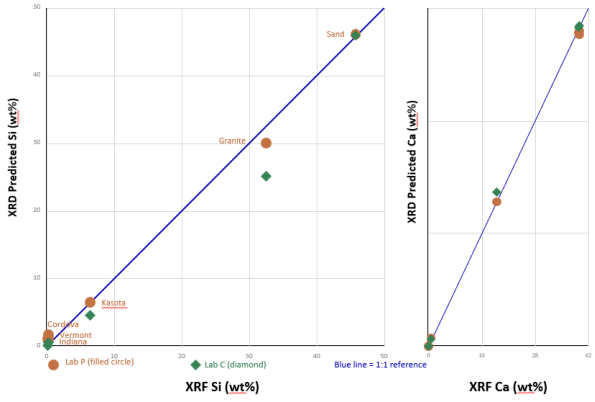

Fig. 8. Cross-plot of XRF-measured Si against XRD-predicted Si (all six samples). Points on or below the 1:1 reference line are acceptable (XRD does not exceed XRF). Points above the 1:1 line indicate mass-balance violations (XRD overestimates minerals containing the element plotted).

With the above cross checking, the following an be summarized:

- XRF vs XRD cross-validation confirms that Lab C provides more physically consistent XRD mineral quantifications than Lab P for the near-pure limestone samples.
- Lab P systematically overestimates quartz by 1.4-2.4%, which propagates to calcite underestimation through XRD normalization.
- Computed grain densities remain within 0.004 g/cm3, about 10 times smaller than the difference observed between reported plug and powder grain densities [4].

4 DISCUSSIONS

4.1 Petrography as the Interpretive Framework

SEM-EDS petrography provides direct unambiguous primary mineral identification prior to bulk powder analyses and reveals features that directly inform interpretation of XRD and XRF data.

For the near-monomineralic calcite samples (Vermont Marble, Cordova Cream, Indiana Limestone), petrography established that detectable quartz should be minimal - sub-percent at most. This visual ground truth, combined with XRF Si constraints, helped to put XRD results in context.

For the Kasota Dolomite, SEM identification of dolomite rhombs with variable Mg/Ca ratios at grain margins was critical context for interpreting mass-balance discrepancies in Mg prediction, pointing to the importance of end-point composition selection.

Petrography is particularly valuable for identifying mixed-mineralogy phases (clay-coated grains, dolomitic calcite, authigenic overgrowths) that can confound XRD peak deconvolution.

This study reinforces the view that petrography should be performed before committing to bulk mineralogical testing, particularly for samples of uncertain or complex lithology.

4.2 XRF Strength and Limitations

WD-XRF offers accurate, reproducible elemental data across a wide dynamic range - from major elements (Si, Ca, Mg, Al, Fe, K, Na at % level) to minor elements at the sub-percent level. The fused-bead preparation eliminates particle-size and mineralogical matrix effects, providing reliable bulk elemental data independent of mineral identification assumptions. CRM verification confirmed excellent accuracy (deviation less than 0.1% for major oxides).

XRF cannot directly identify mineral phases or distinguish polymorphs with identical elemental compositions (e.g., calcite vs. aragonite; quartz vs. cristobalite). Conversion of XRF oxide data to elemental composition is a simple process that makes cross-validation with XRD easier.

In practice, XRF is applied as a cross-check for XRD, and can be used along with XRD to derive element-to-mineral associations for more accurate mineral characterization.

The rule that XRD-derived elemental fractions should not exceed XRF values is a powerful and practical QC tool for end-users.

4.3 XRD Quantification Challenges

Several quantification challenges were identified in this study:

Quartz over-quantification in carbonates: Lab P systematically reported 1.4-2.4% more quartz than the XRF Si constraint allows in near-pure limestone samples. This may reflect background correction artifacts, peak

overlap at very low phase concentrations (less than 3%), or RIR method limitations for minor phases. The XRF cross-check is essential for detecting this artifact.

Normalization propagation: Because XRD results normalize to 100%, overestimation of one phase (such as quartz) produces compensating underestimation of another (such as calcite). This explains why Lab P's calcite values are consistently 1-2% lower than Lab C for the limestone samples.

Clay quantification variability: Even where bulk mineral assemblages agree, clay speciation (illite vs. smectite vs. mixed-layer) varies between laboratories due to differences in glycolation conditions, size-fraction cutoffs, and mixed-layer simulation software. For applications where clay type affects cation exchange capacity [5,6] and swelling potential, this variability has practical consequences.

Granite sampling heterogeneity: For coarse-grained rocks (greater than 1 mm grain size), representative subsampling for XRD requires a large sample mass or rigorous splitting. The inter-laboratory Si discrepancy of approximately 10% in granite most likely reflects physical sampling bias rather than analytical error. For best results, all samples should be homogenized prior to splitting for XRD and XRF analysis.

Dolomite end-point sensitivity: XRD-calculated Mg exceeds XRF Mg by both labs on Kasota Dolomite (Lab P: 10.93% vs. XRF 10.33%; Lab C: 11.61%). This suggests the ideal dolomite end-point overestimates Mg, possibly due to partial Fe substitution in the Mg cation sites, reducing the effective Mg/Ca ratio.

Collaborative determination of dolomite end-point compositions with the XRD laboratory is recommended for high-accuracy carbonate characterization.

4.4 FTIR Applicability

FTIR in ATR mode reliably determined principal mineral groups (carbonate vs. silicate; calcite vs. dolomite) and showed high measurement reproducibility. However, FTIR could not quantify minor mineral phases below approximately 3-5% in the presence of dominant absorbers and could not differentiate quartz from feldspar quantitatively in the complex granite spectrum.

Therefore, commercial FTIR services should not be used as a standalone quantitative mineralogy tool for reservoir characterization at the required precision levels. Its primary value is as a low-cost, rapid screening step - useful for batch screening before full XRD analysis, for anomaly detection (unexpected sulfate or phosphate peaks), and for confirming dominant carbonate mineralogy. Accuracy improves with formation-specific calibrations.

4.5 Integrated Workflow and Best Practices

Recommended Mineralogy Testing Protocol

Based on this comparative analysis, the following sequential workflow is recommended for end-users of commercial mineralogy testing services (Fig. 9):

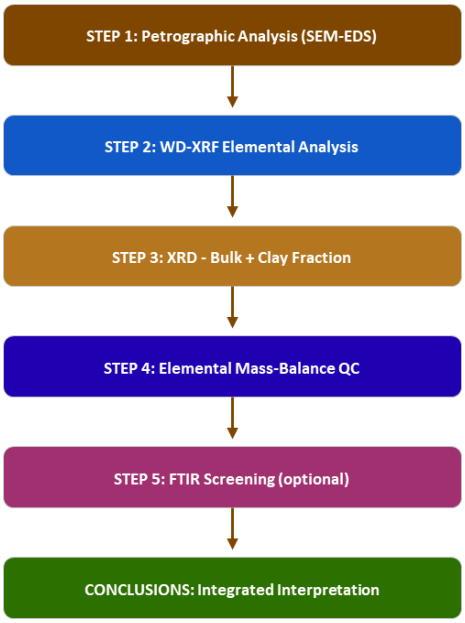

Fig. 9. Integration workflow and best practice.

Step 1 Petrographic analysis (SEM-EDS or optical thin section): Establish mineral ground truth, assess rock fabric and heterogeneity, identify clay morphology, and prioritize targets before committing to bulk powder methods.
Step 2 Preparation: Gently disaggregate and grind enough sample material to provide homogenous splits for XRF and XRD analysis.
Step 2 WD-XRF: Obtain bulk elemental data as an independent, model-free constraint for subsequent XRD cross-validation.
Step 3 FTIR *(optional):* Apply as a rapid confirmatory group-level check and for batch screening prior to full XRD analysis.
Step 4 XRD (bulk plus clay fraction): Request full bulk and clay-fraction mineral quantification. Also request raw diffractogram files and fitting reports - not just tabulated results - to enable independent review and QC.
Step 5 Elemental mass-balance QC: Compare XRD-calculated elemental wt% with XRF results. Flag any data where XRD-predicted elemental fractions exceed XRF values. Use guidance from XRD interpreter on values for mineral endpoints (i.e. Fe substitution in dolomite.)

XRD Report QC Recommendations

Practical QC checkpoints for end-users when reviewing commercial XRD reports:

1. Request laboratory method descriptions, including instrument, software, sample preparation, etc.
2. Verify that XRD totals sum close to 100%. Systematic deviation suggests calibration issues.
    a. Understand that, if organics are present, renormalization with measured organics is

required for most accurate results because XRD does not quantify organics.

3. Apply quartz constraint: Compare SiO2 from XRF to Quartz from XRD. The amount of Quartz will almost always be lower than the SiO2 from XRF, but it should never exceed it within instrument uncertainties.
4. Apply Mg-dolomite constraint: Multiply the amount of dolomite in wt.% by 0.132. This result should be less than or equal to Mg from XRF.
5. Ensure clay speciation patterns include glycolated mount analysis - air-dried analysis alone is insufficient for mixed-layer clay characterization.
6. Request duplicate measurements on at least one representative sample per lithotype to characterize analytical repeatability.

5 Conclusions

This mineralogy comparative study using WD-XRF, XRD, and FTIR for six well-characterized outcrop samples yields the following principal conclusions:

Petrography (SEM-EDS) is an indispensable interpretive guide for all other indirect mineralogical testing methods. It provides a visual understanding of mineral relationships and improves understanding and enables integration of XRD and XRF results within a matrix framework. Seeing the rock provides the ground truth needed to evaluate the physical plausibility of bulk analytical results.

WD-XRF provides robust elemental data serving as an independent cross-check for XRD mineralogy. The rule that XRD-derived elemental fractions cannot exceed XRF values within instrument uncertainty is a powerful and practical QC tool for end-users. Simple comparisons of quartz with SiO2 (Fig. A1) and dolomite with Mg (Fig. A2) provide quick first-glance validation.

FTIR is the most valuable as a rapid, cost-effective screening tool for dominant mineral group identification, not as a standalone quantitative mineralogy method unless specifically calibrated for relevant formations.

XRD is the primary quantitative mineralogy tool but exhibits systematic inter-laboratory differences. If a laboratory over-estimates a mineral, not supported by XRF, this propagates to the underestimation other minerals because of results normalization.

Clay quantification and speciation show inter-laboratory variability due to differences in preparation protocols and software used. Close collaboration with laboratory specialists is essential for reliable clay-typing and quantification.

Quantification of Mg- and Fe-carbonate substitutions from XRD is a key limitation of the XRD technique: small errors in dolomite end-point composition (ideal dolomite vs. Fe-bearing dolomite) produce measurable mass-balance discrepancies, that can affect results of formation evaluation and reservoir characterization.

The impact of inter-laboratory XRD differences on computed grain density is small for near-pure carbonates (0.002-0.004 g/cm3). However, systematic errors in major phase quantification in mixed-mineralogy formations could produce more significant petrophysical deviations.

The most reliable mineralogical interpretations result from integrating petrography, XRF, XRD, and FTIR within a systematic mass-balance framework. This requires active engagement between end-users and laboratory experts rather than passive outsourcing.

6 Acknowledgment

We would like to thank colleagues at partner laboratories who performed the reported tests and provided detailed test protocols, including Gerardo Torrez, Lab P, Lab C, Stratum Reservoir, Corespec, RohmTek.

7 Nomenclature

ATR: attenuated total reflectance
CRM: certified reference materials
FTIR: Fourier-transform infrared spectroscopy
LOI: Loss on ignition
MIR: mid-infrared radiation
RIR: Reference Intensity Ratio ()
SEM-EDS: scanning electron microscopy with energy-dispersive X-ray spectroscopy
WD-XRF: wavelength dispersive X-ray fluorescence
XRD: X-ray diffraction

8 References

1. M. Al-Hamad, A. AlRadhwan, O. Sindt, S. Ma. Obtaining Grain Density of Carbonate Rocks: Core Plugs and Powder Samples, SPE-227052-MS, MEOSGEO, 16-18 Sept (2025)
2. S. Al-Ofi, S. Ma, and G. Jin. Resolving Challenges in Analyzing Iron-Rich Samples by X-Ray Diffraction, The 36th International Symp of the Society of Core Analysts, Abu Dhabi, 9-12 Oct (2023)
3. S. Ma and M. Amabeoku. Core analysis with emphasis on carbonate rocks- quality assurance and control for accuracy & representativeness, *Journal of Interpretation*, Feb (2015)
4. S. Ma, A. Al-Muthana, and R. Dennis. Use of core data in log lithology calibration. SPE-77778-MS, SPE ATCE, Sept (2002)
5. A. Alkhaldi, T. Okasha, and S. Ma. Measurement of cation exchange capacity -a lab comparative study, SPE-227122-MS, MEOSGEO, 16-18 Sept (2025)
6. M. Al-Hamad, S. AlHarbi, A AlZoukani, and S. Ma. Factors affecting lithium adsorption on clay minerals, paper SCA 2026-031, SCA Annual Symposium, Mexico City, Mexico, August 17-21 (2026)
7. H.M. Rietveld, A Profile Refinement Method for Nuclear and Magnetic Structures, J. Appl. Crystallogr., vol. 2, pp. 65-71 (1969)

8. R.C. Reynolds Jr., NEWMOD: A Computer Program for the Calculation of One-Dimensional Diffraction Patterns of Mixed-Layered Clays, R.C. Reynolds, Hanover, NH (1985)

9. G.W. Brindley, G. Brown (Eds.), Crystal Structures of Clay Minerals and Their X-ray Identification, Mineralogical Society, London (1980)

10. R. Jenkins, R.L. Snyder, Introduction to X-ray Powder Diffractometry, Wiley, New York (1996)

11. M. Hillier, Accurate Quantitative Analysis of Clay and Other Minerals in Sandstones by XRD: Comparison of a Rietveld and an RIR Method and the Importance of Sample Preparation, Clay Minerals, vol. 35, pp. 291-302 (2000)

12. B.D. Cullity, S.R. Stock. Elements of X-ray Diffraction, 3rd ed., Pearson Education, New Jersey (2001)

13. M.J. Wilson. The Origin and Formation of Clay Minerals in Soils: Past, Present and Future Perspectives, Clay Minerals, vol. 34, pp. 7-25 (1999)

14. D.L. Bish, J.E. Post (Eds.). Modern Powder Diffraction, Reviews in Mineralogy Vol. 20, Mineralogical Society of America, Washington, D.C. (1989)

15. J. Schon. Physical Properties of Rocks: Fundamentals and Principles of Petrophysics, Elsevier, Oxford (2011)

9 Appendix -

Converting XRF oxides to elements:

XRF analysis measures the dry weight percent of elements in a sample, but the results are usually reported as oxides. To compare results to other measurements, a conversion from oxide back to elements is required. This is done based on the mass of each oxide. The mass percent of the element is simply derived as a percentage of the total mass, as showing below using SiO2 as an example:

Example of SiO2

- Si atomic weight = 28.09 g/mol
- O atomic weight = 15.99 g/mol

Because SiO2 has 1 mol of Si and 2 mol of O, total atomic weight can be calculated as

- SiO2 atomic weight = 28.09 + 2*15.99= 60.07 g/mol

Thus, as exampled in Table 2 for oxides, contribution of Si to SiO2 weight = 28.09/60.07= 0.4676.
To convert oxide SiO2 to element Si in wt%, multiplying the wt.% of SiO2 by 0.4676 to get the wt.% of Si.
A more general form of the above may be written as

$$W_i^{XRF} = \sum_1^{n\_o} XRF_O C_{O,i} \quad \text{(A1)}$$

Where XRF_O is the wt% of oxide $C_{O,i}$ is the conversion constant for element i in oxide O, and W_i^{XRF} is the wt% of element i derived from XRF results.

Converting XRD minerals to elements

It is possible to calculate, within reasonable estimation, the total elemental composition from XRD mineral weight percentages, using Eq 1. This requires some assumptions in endpoint mineral compositions, particularly for minerals such as clays that have varying stoichiometry, but even with those assumptions, this process provides strong cross-validation of results, as shown by the below simple example.

Example of a Simple Rock

The example rock has 70% quartz, 20% kspar and 10% calcite. Given the below endpoint compositions for each mineral (Table 2), the elements wt% can be calculated using Eq. 1.

Name	Si	Al	Ca	K
Quartz	0.467	0	0	0
K-spar	0.303	0.097	0	0.140
Calcite	0	0	0.400	0

- Total Si =70*0.467+20*0.303 = 38.75 wt%
- Total Al = 20*0.097 = 1.94 wt%
- Total Ca = 10*0.400 = 4.00 wt%
- Total K = 20*0.140 = 2.80 wt%

These calculated elemental values can then be compared to the measured elemental values from XRF (converted from oxide form) for cross validation.

Each mineral chosen in this example has consistent chemical compositions. Discrepancies between XRD and XRF can occur when minerals with varying compositions, such as clays, are included.

Quick-look validation of XRD and XRF results:

Example of quartz

A quick way to check XRF and XRD agreement is to plot Quartz from XRD on the Y-axis and SiO2 from XRF on the X-axis, and add a one-to-one (1:1) line. Because quartz is SiO2, the two can be directly compared with the below QC tip:

- No samples should locate above the 1:1 line
  - because it is not possible to have more quartz than there is SiO2.
  - It is, however, likely to have more SiO2 than quartz, because of the presence of other silicate minerals.

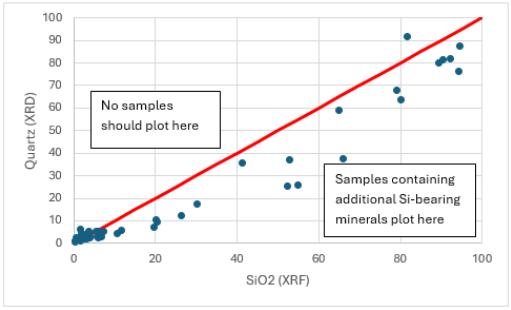

Fig. A1. QC of XRD and XRF data: a sandstone example.

Example of dolomite

Similarly, for a quick XRD dolomite mineral to XRF Mg element comparison, the easiest is to have a quick calculation of how much Mg is being contributed by the dolomite by multiplying it by 0.132 (Table 2), then plotting this against measured XRF Mg.

- Again, data should not normally plot above the 1:1 line, but samples with other Mg-bearing minerals, especially chlorite, will plot below the 1:1 line.

In the below example, some samples plot slightly above the line; could be due to Fe substitution in the dolomite.

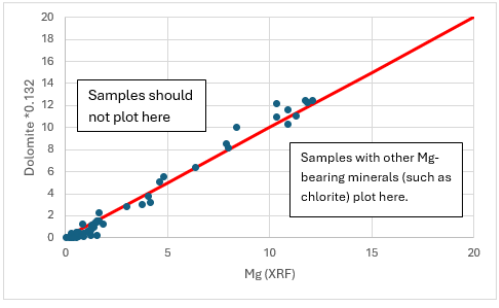

Fig. A2. QC of XRD and XRF data: a dolomite example.